

# LONGITUDINAL BEAM DYNAMICS IN FRIB AND REA LINACS

A. S. Plastun†, P. N. Ostroumov, A. C. C. Villari, Q. Zhao

Facility for Rare Isotope Beams, Michigan State University, 48824, East Lansing, Michigan, USA

## Abstract

The Front-End and first three cryomodules of the Facility for Rare Isotope Beam (FRIB) at Michigan State University (MSU) commissioned in July, 2018. The paper describes the online tuning procedures of the longitudinal beam dynamics through the FRIB linac. These procedures include tuning of the accelerating field phases and amplitudes in the cavities. We developed an automated simulation-based tuning procedure for the multi-harmonic buncher. In order to tune the radio-frequency quadrupole (RFQ) we measured and calculated its threshold voltage and scanned its longitudinal acceptance. Tuning of the rebunchers and superconducting accelerating cavities is performed by means of the phase scans and Time-Of-Flight (TOF) beam energy measurements with beam position and phase monitors.

While FRIB is being commissioned, the re-accelerator (ReA3) for rare isotope beams (RIBs) is being upgraded. We redesigned the ReA3 RFQ to improve its cooling system and provide reliable operation with 16.1 MHz pre-bunched ion beams with  $A/Q = 5$ . In order to provide matching of any ReA3 beam both to the following upgrade cryomodules and physics experiments' requirements, room temperature rebuncher/debuncher is being designed. The design procedure includes the beam dynamics, electromagnetic, thermal and mechanical simulations and optimizations.

## INTRODUCTION

The Facility for Rare Isotope Beams (FRIB) [1] is being built to provide 400 kW ion beams up to uranium for the rare isotope production. The beam will be accelerated by the RFQ and 316 superconducting RF (SRF) cavities to the energy of 200 MeV/u.

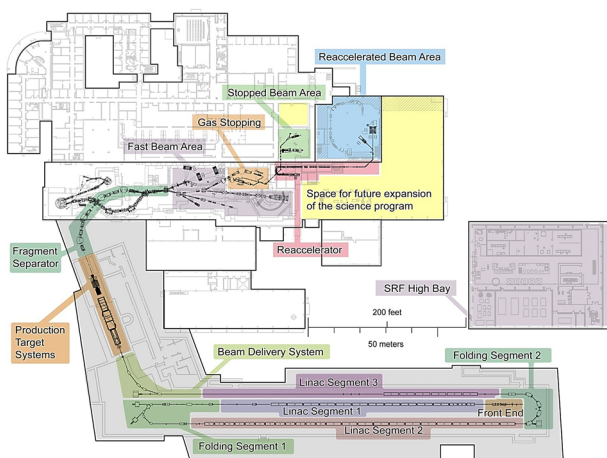


Figure 1: FRIB Layout.

† email address: plastun@frib.msu.edu

The FRIB linac consists of the Front-end and three linac segments (see Fig. 1). The DC beam, created in the ECR ion sources is accelerated to 500 keV/u and injected into the cryomodules of the linac segment 1 (LS1) as shown in Fig. 2 [2]. The 12 keV/u DC beam is pre-bunched by a multi-harmonic buncher to form a small longitudinal emittance. The RFQ is followed by medium energy beam transport (MEBT) to the cryomodules. The MEBT has two room-temperature quarter-wave (QWR) rebunchers to match the beam to the following SRF cavities in the longitudinal phase space.

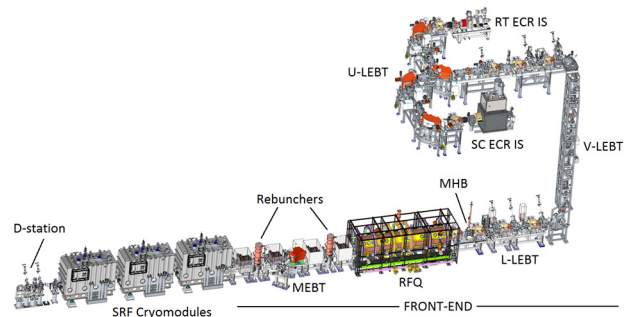


Figure 2: FRIB Front-end and first three cryomodules.

The detailed description of the FRIB linac components is given elsewhere [3-6].

FRIB is designed to accelerate two uranium charge states (33+ and 34+) in LS1 simultaneously, strip them in the liquid lithium stripper and continue acceleration of all five charge states (76+ through 80+) in one RF bucket [4, 5]. Proper tune of field amplitudes and phases of all FRIB cavities, including the bunching ones, is an essential procedure required to provide low losses and low emittance growth of the multi-charge-state beam [6].

## MULTI-HARMONIC BUNCHER

The main purpose of the multi-harmonic buncher (MHB) is to form bunches with a small longitudinal emittance, which is required to maintain low particle losses in the SRF part of FRIB in multi-charge acceleration mode [6]. Also, MHB provides the longitudinal matching of the beam with the RFQ acceptance to maintain small emittance along the RFQ.

The FRIB MHB consists of two resonant quarter-wave lines attached to a pair of conical drift tubes [7]. The long line resonates at frequencies of 40.25 MHz and 120.75 MHz. The short line resonates at 80.5 MHz. Tuning of the MHB is an optimal choice of harmonics amplitudes and phases to provide small longitudinal beam emittance, proper matching with the RFQ and ~80% transmission of the accelerated beam.

Content from this work may be used under the terms of the CC BY 3.0 licence (© 2018). Any distribution of this work must maintain attribution to the author(s), title of the work, publisher, and DOI.

At the time of the Front-end commissioning we didn't have any diagnostic tools to characterize the longitudinal beam emittance. For this reason, we developed a simulation-based tuning approach.

### Simulation-based Tuning of the MHB

The idea of this approach is to find the MHB tune, which could be closely simulated. And then just rescale the amplitudes to provide minimum longitudinal emittance according to the simulation results. Since we could reliably measure the beam transmission through the RFQ, the selected tune was the "maximum transmission tune".

First, we created the electrostatic model of the FRIB RFQ vane tips in CST [8] which is based on the point-to-point tip geometry provided by PARMTEQ [9]. The latter was used to generate the vane tip modulation. Figure 3 shows the 3D model of the vanes. Since the RFQ has voltage increase along the resonator from 60 kV to 112 kV, the 3D-field distribution has been multiplied by the linear  $V(z)$ -law and exported cell-by-cell to use in the beam dynamics simulations. All beam dynamics simulations presented in this paper have been performed with TRACK code [10].

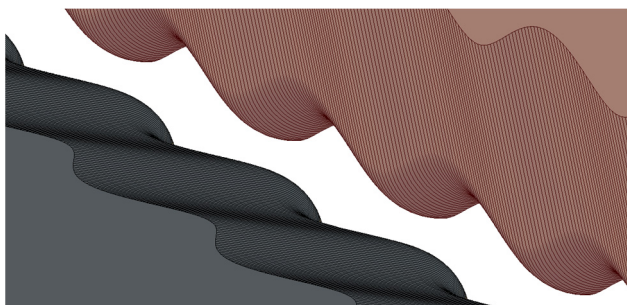


Figure 3: Vane tips of the FRIB RFQ 3D model.

Second, we created the RF and electrostatic models for the MHB in CST. Beam dynamics simulations in the MHB showed that combined 3D electromagnetic field distribution of three harmonics can be replaced by a sequence of three gaps with electrostatic field of charged drift tubes resonating at MHB frequencies, as presented in Fig. 4. The focusing solenoid in front of the RFQ was also added into the TRACK model.

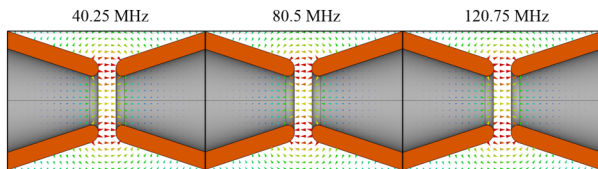


Figure 4: MHB model for beam dynamics simulation.

Finally, we developed the python-based interface to TRACK to enhance optimizing capabilities. Python script using the Nelder-Mead simplex method automatically finds amplitudes of MHB harmonics corresponding to the maximum beam transmission. The MHB settings for "minimum ratio of longitudinal emittance to transmission" and "minimum longitudinal emittance" were found as well. Phase-space plots at the entrance of the RFQ are presented

in Fig. 5. Parameters of the beam exiting the RFQ are summarized in Table 1.

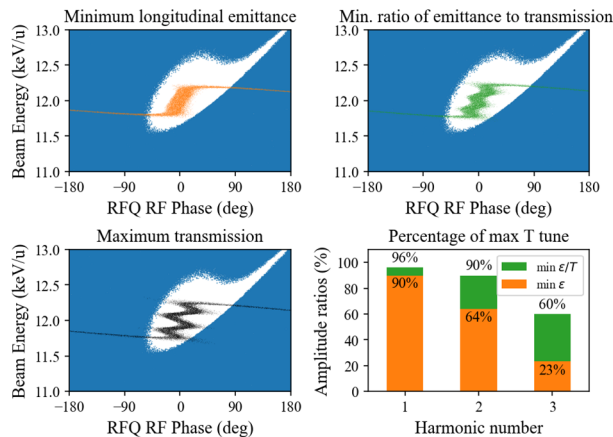


Figure 5: Phase-space plots for MHB tunes and their harmonic amplitudes. White area represents the RFQ longitudinal acceptance.

Table 1: Beam Parameters After the RFQ

MHB Tune	Long. emittance, rms ( $\pi \cdot \text{keV}/u \cdot \text{ns}$ )	RFQ+MEBT Transmission (%)
Max T	0.103	83.8
Min $\epsilon/T$	0.079	81.6
Min $\epsilon$	0.074	76.3

FRIB control system is built on Experimental Physics and Industrial Control System (EPICS) [11]. We widely use python *epics* package to get data and control the accelerator. In order to tune the real MHB for maximum transmission we developed the python script scanning the amplitudes and phases of harmonics. The highest transmission can be achieved in two-three iterations of phase-amplitude sweep. Other MHB tunes are set by scaling the amplitudes as shown in Fig. 5.

During the commissioning of the first three cryomodules we performed the SRF cavity amplitude scan and measure the bunch length at each field level. Scan result were used to reconstruct the longitudinal beam emittance after the acceleration by seven SRF cavities. The measured (reconstructed) and simulated emittances are presented in Table 2.

Table 2: Longitudinal rms Beam Emittance

MHB Tune	Simulated emittance ( $\pi \cdot \text{keV}/u \cdot \text{ns}$ )	Measured emittance ( $\pi \cdot \text{keV}/u \cdot \text{ns}$ )
Max T	0.14	0.19
Min $\epsilon$	0.12	0.14

## RADIO-FREQUENCY QUADRUPOLE

The first faraday cup (FC) downstream the FRIB RFQ is located behind the third quadrupole triplet of the MEBT. The non-accelerated particles are lost upstream of the FC.

Content from this work may be used under the terms of the CC BY 3.0 licence (© 2018). Any distribution of this work must maintain attribution to the author(s), title of the work, publisher, and DOI.

This fact allows us to measure the RFQ threshold voltage [12, 13]. Comparing the calculated and measured values for the threshold voltage we can set the design field level in the RFQ. The relationship of the design  $V_0$  and threshold  $V_{th}$  voltages is:

$$\frac{V_{th}}{V_0} = \cos\varphi_s, \quad (1)$$

here  $\varphi_s$  is the synchronous phase in the regular part of the RFQ, which is equal to  $-25^\circ$  for the FRIB RFQ. It results in  $V_{th} = 63$  kV at  $V_0 = 69.5$  kV for  $^{40}\text{Ar}^{9+}$  used for the measurements of the threshold curve (see Fig. 6).

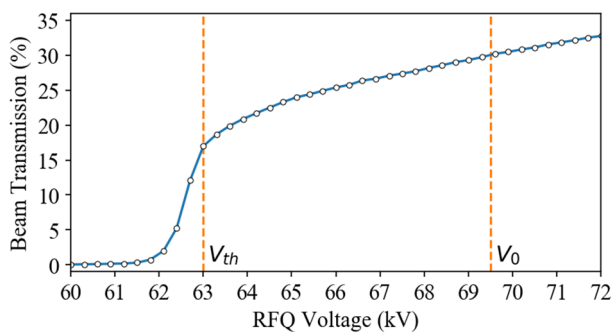


Figure 6: Threshold curve of the FRIB RFQ. Horizontal axis represents the maximum RFQ voltage along the resonator.

This procedure for the accelerating field calibration is widely applied to drift tube linacs (DTLs) with magnetic focusing, such as an Alvarez-DTL. But it cannot be used with an RFQ if one measures the output beam current right at the RFQ exit, because fraction of non-accelerated beam is usually high.

Another way to check the field setting of the RFQ is the energy scan of the longitudinal acceptance. We created a script, which sweeps the DC beam energy, scales the LEPT optics according to equations below and measures the RFQ+MEBT beam transmission:

$$\frac{V}{V_{des}} = \frac{W}{W_{des}}, \quad \frac{I}{I_{des}} = \frac{v}{v_{des}}, \quad (2)$$

here  $V$  are voltages of electrostatic quadrupoles and e-bends and  $I$  are currents of magnets,  $W$  is the beam energy,  $v$  is the beam velocity. Index *des* means design value corresponding to the energy of 12 keV/u. The result of the energy scan is presented in Fig. 7. In the simulation we used 4D-Gaussian distribution with rms emittance of  $0.12 \pi \cdot \text{mm} \cdot \text{mrad}$ . Since the simulated and measured energy profiles agree very well, we believe that the RFQ voltage is set correctly at  $V_0 = 69.5$  kV.

RF Phase of the RFQ relative to the FRIB global timing system is always equal to  $0^\circ$ . All other cavities, including the MHB, have to be properly phased relative to the beam.

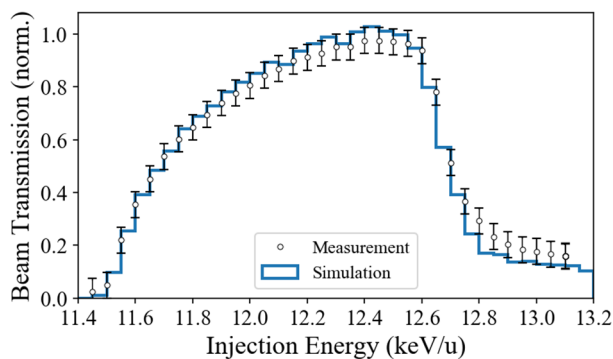


Figure 7: Energy scan of the RFQ longitudinal acceptance.

## CAVITY PHASE SCAN

Phase scan of the cavities includes measurement of the phase and amplitude of the signal from the beam position monitors (BPMs) next to the cavity. Phase of the signal is a function of the time of flight from the cavity to the BPM. The lowest phase corresponds to the highest beam velocity, i.e. to the cavity phase for maximum acceleration. The design accelerating phase is calculated from the phase of maximum acceleration. Figure 8 shows the result of a cavity phase scan. Measured points are interpolated with cubic splines and maximum acceleration phase is calculated ( $124^\circ$  in the Fig. 8). The accelerating phase is equal to  $94^\circ$  in this plot and corresponds to  $-30^\circ$  synchronous phase.

The cavity accelerating fields are adjusted to match the design energy gain. Beam energy is automatically calculated online from the measured phases of BPMs' signals.

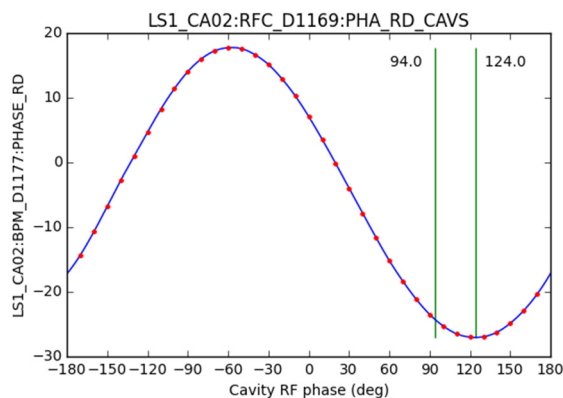


Figure 8: Example of the cavity phase scan result. Vertical axis is a phase of the signal from the BPM next to the cavity.

During the first three cryomodule commissioning phase scans were performed at 20% of the design cavity field level to avoid strong RF defocusing and steering of the misaligned beam. A phase scan procedure takes about 1 minute, beam trajectory correction takes 1 – 10 minutes (longer for the first several cavities) and about 3 minutes are required to ramp up the cavity field to the design amplitude. The LS1 commissioning scheduled for the spring 2019 will include phase scans of 88 SRF cavities. We are developing the python application to scan the cavities one-

by-one automatically including turn-on procedures and field ramp-up. Our current goal is 60 seconds per cavity.

### Rebuncher Phase Scan

If the cavity is a rebuncher the operating phase is then defined as a cross-point of two curves measured at two different field levels as shown in Fig. 9. BPM magnitude signal is used to figure out which of two cross-points is bunching (i.e.  $-90^\circ$  from the maximum acceleration phase) and which is debunching (i.e.  $+90^\circ$  from the maximum acceleration phase). Buncher voltage is calibrated by energy measurement at the phase of maximum acceleration.

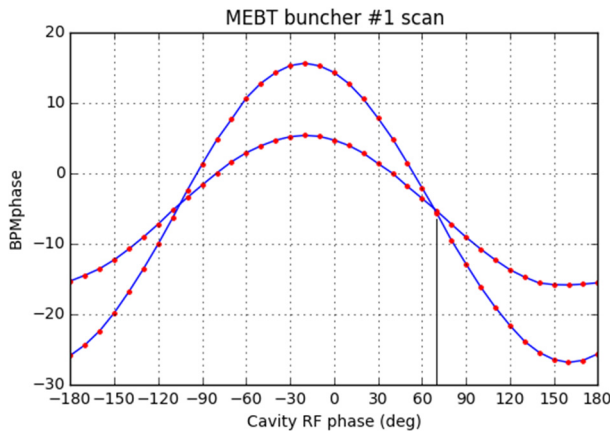


Figure 9: Example of the buncher phase scan result.

## RE-ACCELERATOR UPGRADE

While FRIB is being commissioned, the MSU re-accelerator (ReA) for rare isotope beams (RIBs) is being upgraded. ReA was commissioned as ReA3 in 2015 [14] and currently accelerates rare isotope beams with charge-to-mass ratio from 0.25 to 0.5 at the energy range from 0.3 to 6 MeV/u. The ReA3 upgrade includes: (a) replacement of the ReA3 RFQ electrodes to improve the cooling and to provide higher capture efficiency for 16.1 MHz bunches with charge-to-mass ratio down to 0.2, (b) adding another three cryomodules after the ReA3, (c) installation of the new electron beam ion trap (EBIS), (d) new RF controllers. Upgraded ReA options called ReA6 and ReA12 will significantly extend the scientific program allowing to reach beam energies up to 24 MeV/u (see Fig. 10).

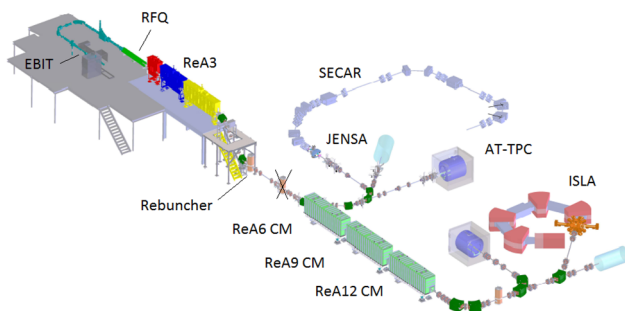


Figure 10: MSU Re-accelerator layout.

In order to match any ReA3 beam to the following upgrade cryomodules and meet the requirements of low energy nuclear physics experiments', a room temperature cw rebuncher/debuncher will be developed and built.

### ReA3 RFQ Upgrade

To provide the reliable cw operation of the ReA3 RFQ the electrodes were re-designed to reduce the inter-vane voltage from 86.5 kV to 70 kV, peak fields from 1.6 to 1.45 Kilpatrick units, RF power consumption from 160 kW to 100 kW. The RFQ resonator and, consequently, the length of the electrodes remains the same. To gain more energy at reduced voltage we implemented the trapezoidal modulation of the electrodes in the acceleration section of the structure. Currently, no RFQ-design codes capable of designing the electrodes with both sinusoidal and trapezoidal modulation are available. To deal with it we developed the practical design approach for RFQs [15]. It is based on a VBA Macro running in CST STUDIO and performing the cell-by-cell construction of the 3D CAD model for the modulated electrodes. The macro automatically adjusts the cell lengths to match the desired synchronous phase law. Each iteration consists of electrostatic simulation of the CAD model, 1D beam dynamics simulation of the reference particle, evaluation of the RF phase in the cell center and adjustment of the cell length if needed. At the end of the design procedure we generated the CAD model which was used for the electrodes' fabrication. The photo of the machined electrodes is shown in Fig. 11. The installation is scheduled for 2019.

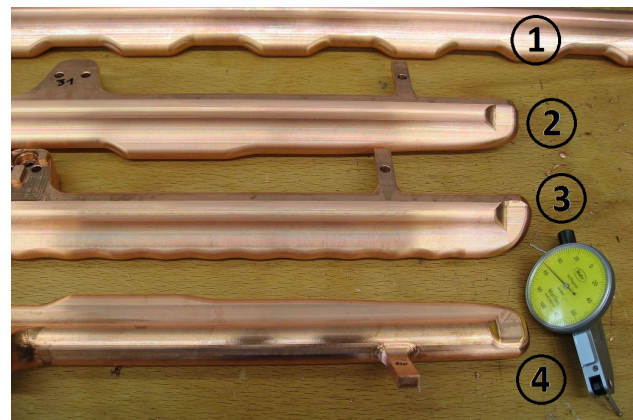


Figure 11: Manufactured electrodes for ReA3 RFQ Upgrade (provided by Kress GmbH, Germany). #1 – trapezoidal part, #2 and #4 – output radial matcher, producing round beam, #3 – input radial matcher and sinusoidal part.

### Rebuncher

The main purpose of the rebuncher is to match ReA3 beams with the energy of  $12 \cdot Q/A$  MeV/u to the ReA6 cryomodule, here  $Q$  is an ion charge state and  $A$  is an ion mass number. Another function of the rebuncher is to debunch 0.3 – 6.0 MeV/u beams for ReA3 users. The requirement for the bunch length is  $\pm 1$  ns and for the energy spread is  $\pm 1$  keV/u. We have studied several options: 80.5 MHz or

Content from this work may be used under the terms of the CC BY 3.0 licence (© 2018). Any distribution of this work must maintain attribution to the author(s), title of the work, publisher, and DOI.

161 MHz cavity, single rebuncher in two different locations or two rebunchers, double-gap QWR and multi-gap IH structure, etc. The main criteria were low construction and operational costs. Figure 12 shows the basic design of the rebuncher cavity. Its parameters are presented in Table 3.

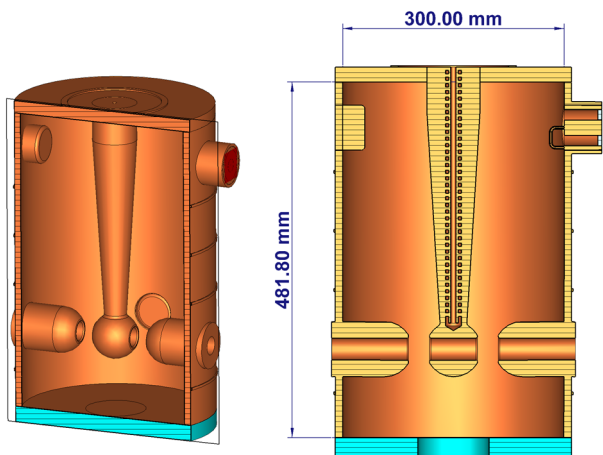


Figure 12: ReA rebuncher design.

Design of cw cavities usually includes coupled RF, thermal and mechanical simulations due to high heat load from RF losses. Multiphysics design of the cavity is fully completed with a combination of CST STUDIO and SolidWorks Flow Simulation Tool. The latter is mostly used to calculate the heat transfer coefficients for water cooling channels.

Table 3: ReA Rebuncher Parameters

Parameter	Value	Unit
Frequency $f_0$	161	MHz
$\beta_G$	0.1	
Voltage $V_0$	200	kV
RF power $P_0$	4	kW
Quality factor $Q_0$	13,000	
Peak surface field $E_{peak}$	0.6	Kilpatrick units

## ACKNOWLEDGMENTS

Authors would like to thank our colleagues for their help with the experiments: T. Maruta, T. Yoshimoto, H. Ren, J. Stetson, S. Renteria, G. Machicoane, E. Pozdeyev, C. Morton, S. Cogan, S. Lidia, S-H. Kim, S. Zhao, and many other physicists and engineers of FRIB. Authors thank B. Mustapha from ANL for the support with TRACK code.

This material is based upon work supported by the National Science Foundation under Grant No. PHY-1565546.

## REFERENCES

[1] J. Wei *et al.*, “The FRIB Superconducting Linac: Status and Plans”, in *Proc. LINAC’16 Conf.*, East Lansing, MI, USA, Sep. 2016, paper MO1A01, pp. 1.

[2] E. Pozdeyev, “FRIB Front End construction and commissioning”, in *Proc. IPAC’18 Conf.*, Vancouver, Canada, May 2018, paper MOZGBF1, pp. 58.

[3] T. Xu *et al.*, “Progress of FRIB SRF Production”, in *Proc. SRF’17 Conf.*, Lanzhou, China, July 2017, paper TUXAA03, pp. 345.

[4] P.N. Ostroumov and K.W. Shepard, *Phys. Rev. ST Accel. Beams*, vol. 3, pp. 030101 (2000).

[5] R. C. York *et al.*, “Beam dynamics in the FRIB linac”, in *Proc. HB’10 Conf.*, Morschach, Switzerland, Sept. 2010, paper TUO1B05, pp. 319.

[6] Q. Zhao *et al.*, “FRIB accelerator beam dynamics design and challenges”, in *Proc. HB’12 Conf.*, Beijing, China, Sept. 2012, paper WEO3B01, pp. 404.

[7] J. Holzbauer *et al.*, “Electromagnetic design of a multi-harmonic buncher for the FRIB driver linac”, in *Proc. PAC’11 Conf.*, New York, NY, USA, Mar. 2011, paper TUP091, pp. 1000.

[8] CST Studio Suite, <http://www.cst.com>

[9] K. R. Crandall *et al.*, “PARMTEQ-RFQ Design Codes”. Los Alamos National Laboratory report LA-UR-96-1836.

[10] The beam dynamics code TRACK. <http://www.phy.anl.gov/atlas/TRACK>

[11] EPICS. <http://www.aps.anl.gov/epics/>

[12] W. Panofsky, “Linear accelerator beam dynamics”, Lawrence Rad. Lab. Rep., UCRL report 1216, 1951.

[13] I.M. Kapchinskiy, *Theory of resonance linear accelerators*, Harwood, 1985.

[14] A. Villari *et al.*, “Commissioning and first accelerated beams in the reaccelerator (ReA3) of the National Superconducting Cyclotron Laboratory, MSU”, in *Proc. IPAC’16 Conf.*, Busan, Korea, Mar. 2016, paper TUPMR024, pp. 1287.

[15] A. S. Plastun and P. N. Ostroumov, *Phys. Rev. Accel. Beams*, vol. 21, pp. 030102, 2018.